Acta Biomaterialia 10 (2014) 751–760

Contents lists available at ScienceDirect

Acta Biomaterialia

journal homepage: www.elsevier.com/locate/actabiomat

Probing the weak interaction of proteins with neutral and zwitterionic antifouling polymers

Jiang Wu [a,b], Chao Zhao [b], Rundong Hu [b], Weifeng Lin [a], Qiuming Wang [b], Jun Zhao [b], Stephanie M. Bilinovich [c], Thomas C. Leeper [c], Lingyan Li [b], Harry M. Cheung [b], Shengfu Chen [a,*], Jie Zheng [b,*]

[a] State Key Laboratory of Chemical Engineering, Department of Chemical and Biological Engineering, Zhejiang University, Hangzhou 310027, China
[b] Department of Chemical and Biomolecular Engineering, The University of Akron, Akron, OH 44325, USA
[c] Department of Chemistry, The University of Akron, Akron, OH 44325, USA

ARTICLE INFO

Article history:
Received 21 June 2013
Received in revised form 24 September 2013
Accepted 30 September 2013
Available online 8 October 2013

Keywords:
Poly(ethylene glycol) (PEG)
Poly(sulfobetaine methacrylate) (pSBMA)
Antifouling materials
Protein–polymer interaction

ABSTRACT

Protein–polymer interactions are of great interest in a wide range of scientific and technological applications. Neutral poly(ethylene glycol) (PEG) and zwitterionic poly(sulfobetaine methacrylate) (pSBMA) are two well-known nonfouling materials that exhibit strong surface resistance to proteins. However, it still remains unclear or unexplored how PEG and pSBMA interact with proteins in solution. In this work, we examine the interactions between two model proteins (bovine serum albumin and lysozyme) and two typical antifouling polymers of PEG and pSBMA in aqueous solution using fluorescence spectroscopy, atomic force microscopy and nuclear magnetic resonance. The effect of protein:polymer mass ratios on the interactions is also examined. Collective data clearly demonstrate the existence of weak hydrophobic interactions between PEG and proteins, while there are no detectable interactions between pSBMA and proteins. The elimination of protein interaction with pSBMA could be due to an enhanced surface hydration of zwitterionic groups in pSBMA. New evidence is given to demonstrate the interactions between PEG and proteins, which are often neglected in the literature because the PEG–protein interactions are weak and reversible, as well as the structural change caused by hydrophobic interaction. This work provides a better fundamental understanding of the intrinsic structure–activity relationship of polymers underlying polymer–protein interactions, which are important for designing new biomaterials for biosensor, medical diagnostics and drug delivery applications.

1. Introduction

A fundamental understanding of protein–polymer interactions is critically important for the rational design of (multi)functional biomaterials for a wide range of scientific and technological applications. The polymers that interact strongly and selectively with proteins are often used for biosensors, tissue engineering and targeted gene and drug delivery [1–5], and can enhance protein adsorption and aggregation and/or regulate protein conformation and orientation at polymer interfaces. Meanwhile, the polymers having weak or inert interaction with proteins are equally important for the development of stealth and functional materials for antithrombogenic implants, drug delivery carriers and antifouling membranes [6–9]. Generally speaking, for most neutral proteins and polymers, hydrophobic interaction is often considered as a major driving force for protein–polymer interactions. For charged protein–polyelectrolyte complexation, electrostatic interaction is a dominant factor. Intensive studies have generated a wealth of polymers and knowledge for the fundamental understanding of protein–polymer interactions and practical uses in various biological applications [10–16]. However, the structure–function relationship of polymers underlying protein–polymer interactions still remains elusive.

Particularly for the "stealth and antifouling" polymers, interactions between proteins and polymers are often dynamically weak and reversible so that these weak protein–polymer interactions are either often neglected or difficult to detect and distinguish from each other, leading to an incomplete and inaccurate description of the structure–activity relationship of the polymers. Surface plasmon resonance (SPR) and quartz crystal microbalance (QCM) are the two most powerful and commonly used tools to measure the interaction of proteins with polymers coated on a substrate, not in bulk solution. However, such weak, reversible interactions would not be observed by SPR and QCM because weakly adsorbed proteins are very likely to be washed out during washing steps

* Corresponding authors.
E-mail addresses: schen@zju.edu.cn (S. Chen), zhengj@uakron.edu (Jie Zheng).

1742-7061/$ - see front matter © 2013 Acta Materialia Inc. Published by Elsevier Ltd. All rights reserved.
http://dx.doi.org/10.1016/j.actbio.2013.09.038

[17]. Such surface interactions between proteins and modified polymer surfaces strongly depend on surface packing properties (density, roughness and thickness) [9,15,18–23]. Additionally, steric repulsion arising from the compression of long polymer chains on the surface by approaching proteins can also contribute to some "insert" polymer surfaces with high surface density and a long polymer chain [24,25]. But these surface-induced effects do not truly reflect the intrinsic polymer–protein interactions in solution. It is very likely that the low-fouling materials in solution can enhance their resistance to proteins and become "superlow fouling" materials when they form a brush structure on the surface.

Among existing "stealth and antifouling polymers", poly(ethylene glycol) (PEG)-based polymers and zwitterionic-based polymers (e.g. poly(sulfobetaine methacrylate) (pSBMA) and poly(carboxybetaine methacrylate) (pCBMA)) have demonstrated their superlow fouling ability to resist protein adsorption and cell adhesion in vitro [26–28]. Both PEG and pSBMA enable one to achieve much lower protein adsorption from undiluted human blood serum and plasma [15,29]. Such strong protein-resistance capacity is mainly attributed to their strong hydration effect [30–34]. However, the PEGylation of proteins was recently found to dramatically reduce their bioactivity, while the conjugation of zwitterionic polymers with proteins enables one to improve the stability of the proteins and to retain or even improve their bioactivity [28,35–37]. Moreover, PEGylated proteins and drug carriers often induce antibody production and cause "accelerated blood clearance" [38], thus limiting their long-term biomedical applications. Considering that PEG is a neutral amphiphilic polymer while pSBMA is a zwitterionic superhydrophilic polymer, we expect that intermolecular interactions between polymers and proteins should be different, with different driven forces. Such differences in protein–polymer interactions are very likely to account for their different behaviors in in vivo and in vitro applications.

Due to extensive use of PEG and pSBMA in fundamental and practical applications, it is of great interest and fundamental importance to re-examine the weak interaction of these two antifouling polymers with proteins in aqueous solution and to better understand the intrinsic difference of polymer–protein interactions, which could be due to different chemical structures and hydration capacities that are often neglected in the literature. More importantly, unlike undetectable protein interactions with PEG as reported in other works, our recent low field nuclear magnetic resource (NMR) results have shown that PEG of high molecular weight (MW > 2000) is not inert in undiluted human blood, and PEG indeed interacts with BSA and LYZ at a measurable level [39]. Such PEG–protein interaction cannot be fully neglected, particularly in a blood circulatory system, because a layer of weakly adsorbed plasma proteins on PEG can still induce the thrombotic and inflammatory reactions at clinical conditions. Motivated by inconsistent data for PEG–protein interactions in the literature, here we characterized and compared the interactions of neutral PEG and zwitterionic pSBMA with model proteins of bovine serum albumin (BSA) and lysozyme (LYZ) using tryptophan fluorescence, 1-anilino 8-naphthalene sulfonic acid (ANS) fluorescence, atomic force microscopy (AFM) and NMR. The effects of protein:polymer mass ratio on protein–polymer interactions were also examined. Tryptophan fluorescence and ANS fluorescence were used to determine the existence of interactions between proteins and polymers. AFM was used to monitor morphological changes of proteins, which qualitatively reflects the structural change of proteins induced by polymers. Proton NMR spectroscopy was used to identify the preferred binding motifs at the surface of lysozyme upon interacting with PEG or pSBMA. Collective data demonstrated that PEG had a weak, reversible hydrophobic interaction with proteins, while pSBMA had an undetectable interaction with proteins. This work gains some fundamental insight into antifouling mechanisms involving rather weak protein–polymer interactions, which hopefully help to rationally design new effective antifouling polymers.

2. Materials and method

2.1. Materials

PEG with molecular weight 20,000 (PEG20000), the monomer, N-(3-sulfopropyl)-N-(methacryloxyethyl)-N,N-dimethylammonium betaine (pSBMA, $H_2C–C(CH_3)–COOCH_2CH_2N(CH_3)2(CH_2)3SO_3$) and the initiators, sodium metabisulfite (SBS), ammonium persulfate (APS), 1-anilino 8-naphthalene sulfonic acid (ANS), BSA and LYZ were purchased from Sigma–Aldrich (Milwaukee, WI). Stock solution of both proteins were prepared with the concentration of 4 mg ml^{-1}. Water used in these experiments was purified by a Millipore water purification system with a minimum resistivity of 18.0 MΩ cm. D_2O (99.9 atom% D) used in experiments was purchased from J&K Chemical.

2.2. pSBMA synthesis

Redox initiators SBS (0.6%, w/v) and APS (1.6%, w/v) were dissolved in 5 ml of mixed water and ethanol (volume ratio 1:1 followed by the addition pSBMA (1.8861 g). The mixture was then placed in a water bath at 38 °C for 1 h and quenched at −20 °C for 30 min. The resultant copolymer was placed in a 3000 g mol^{-1} MWCO cellulose acetate dialysis bag to remove excess monomers and initiators for two days with pure DI water, followed by the lyophilization for 1 day of the solution to obtain pSBMA powder.

2.3. Fluorescence spectroscopy

Steady-state fluorescence experiments were carried out with a LS55 spectrofluorimeter (PerkinElmer, USA). Fluorescence spectra were measured upon adding different amounts of polymers to a fix protein solution of 20 μg ml^{-1}. Polymer concentrations were varied from 0 to 0.5, 1, 2, 4, 8 and 16 (mass ratio of polymers vs. proteins). Intrinsic fluorescence spectra were recorded between 310 and 400 nm with an excitation wavelength of 295 nm, where the contribution of tyrosine residues is negligible. Excitation and emission slit with a nominal 6 nm bandwidth.

ANS is a dye whose fluorescence is greatly enhanced on binding to hydrophobic surfaces, displaying a characteristic blue shift in its fluorescence maximum from ~515 to ~475 nm. During the folding or unfolding process of proteins, exposure of hydrophobic patches could be characterized by this blue shift. For ANS experiments, samples were excited at 350 nm, and emission was scanned between 400 and 600 nm. The wavelength of maximum emission was recorded and plotted against time. The molar ratio of protein to ANS was 1:100, the protein concentration is the same with Trp experiments, 20 μg ml^{-1}, and the polymer concentration is 10:1 (mass ratio of polymers vs. proteins). All experiments were conducted at room temperature.

2.4. NMR

^{1}H-NMR experiments were performed on a Varian INOVA 750 spectrometer. NMR data were routinely acquired at 30 °C. Interaction of polymers (8 mg ml^{-1}) with lysozyme was determined by chemical shift titration from a series of one-dimensional (1-D) NMR experiments using the WATERGATE sequence to suppress the water signal. A series of titration experiments was conducted by changing the polymer:protein mass ratio from 0, 0.5, 1 and 2 to 1, respectively. The solvent is D_2O.

Table 1
The physicochemical properties of polymers (pSBMA and PEG) and proteins (BSA and LYZ).

Polymer	Protein
pSBMA 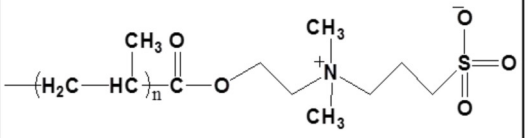 MW 44000 PDI 1.56	BSA^{4F5S} 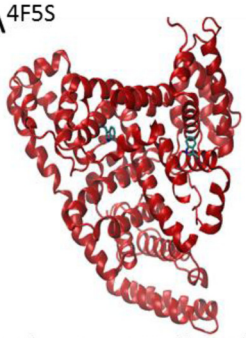 Bovine Serum Albumin-66430Da
PEG20000 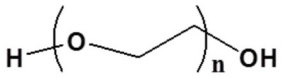 MW 20000 PDI 1.17	LYZ^{1LYZ} 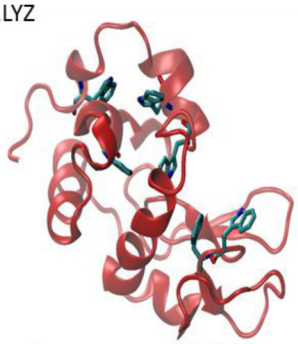 Lysozyme-14400Da

4F5S: PDB (prtotein data bank) code for BSA; 1LYZ: PDB code for LYZ. Trp residues are presented by cyan sticks.

2.5. AFM

Morphological change of proteins in the absence and presence of polymers was imaged by tapping-mode AFM. The freshly peeled highly oriented pyrolytic graphite (HOPG) was soaked into a mixed protein–polymer solution with a protein:polymer mass ratios of 1:10 (protein concentration here is 2 μg ml^{-1}, the solution previously incubated for 24 h) for 20 min, rinsed ten times with 50 μl deionized water to remove any loosely bound polymer and protein and dried for 24 h before AFM imaging. AFM images were acquired using a multimode Nanoscope III equipped with a 15 μm E scanner (Vecco Inc.). Commercial Si cantilever (NanoScience) with an elastic modulus of ~40 N m^{-1} was used. All images were acquired as 512 × 512 pixel images at a typical scan rate of 1.0–2.0 Hz with a vertical tip oscillation frequency of 250–350 kHz. Representative images of each sample were collected by scanning at least five different locations. This AFM protocol is generally used to characterize protein interaction with polymers [40–43].

3. Results and discussion

In this work, two model proteins of BSA and LYZ are used to examine weak interactions with two well-known antifouling polymers of PEG and pSBMA. BSA (66.43 kDa, pI = 4.7) is a negatively charged, large protein, while LYZ (14.4 kDa, pI = 11.3) is a positively charged, small protein under physiological conditions. Both proteins are abundant in the human body, and are typically used to evaluate the nonfouling characteristics of materials due to their roles in the inflammatory response. Table 1 summarizes the basic structural properties of two polymers and two proteins. We should note that a protein interacting with polymer surfaces in the literature is quietly different from a protein interacting with polymers in solution in this study. Numerous works by us and others [11,12,16,18,20,23,27] have demonstrated that apart from polymer chemistry, when the surface is modified by a full layer of polymers, the surface uniformity, density, thickness roughness and even chain length of polymers play a very important role in protein adsorption, but these surface effects will not be presented in the protein interaction with polymer in bulk solution. This work examines the intrinsic property of polymers interacting with proteins in solution by excluding physical surface effects, which can be tuned to control desirable interactions with proteins in an enhanced or reduced way.

3.1. Probing the interaction of proteins with PEG and pSBMA

Steady-state fluorescent spectroscopy of proteins is a proven, rapid and easy method for evaluating protein conformations and protein–polymer association. Here, polymer-induced conformational change of proteins at different polymer:protein mass ratios (0, 0.5, 1, 2, 4, 8 and 16) as a function of time was monitored by the changes in the intensity of tryptophan (Trp) fluorescence (Fig. 1). Specifically, upon a conformational change in protein, tryptophan fluorescence depends not only on the exposure or accessibility of the tryptophan residues, but also on the local protein environment immediately surrounding the tryptophan. In fluorescence experiments, tryptophan was excited at 295 nm with a narrow spectral bandwidth (full width ad half maximum ≈2 nm). At

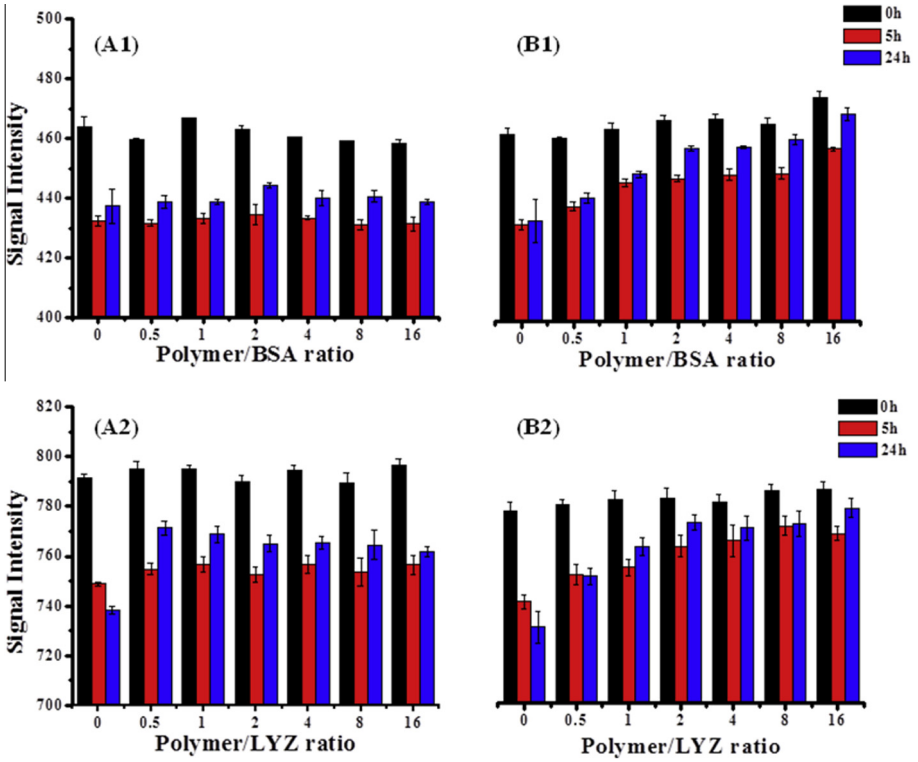

Fig. 1. Effect of polymer/protein mass ratios on the tryptophan fluorescence intensity of proteins at different time points (0, 5 and 24 h) in PBS buffer (pH 7.4) for (A1) pSBMA/BSA, (B1) PEG/BSA, (A2) pSBMA/LYZ, (B2) PEG/LYZ. Error bars represent standard deviation from three independent measurements.

this wavelength, we specifically avoid excitation of other amino acids in the protein, all of which absorb at shorter wavelengths. It can be seen in Fig. 1 that at the very beginning (i.e. 0 h) of protein solutions in the absence and presence of polymers, the intensities of tryptophan florescence were similar to each other and appeared to be independent of the polymer concentrations. This suggests that it takes time for polymers to interact with proteins, if at all, to induce conformation change. As control experiments, in the absence of polymers, pure LYZ or BSA experienced a large fluorescence decrease by ~6–15% at the first 5 h, and then remained unchanged with statistical fluctuation after 5 h. Initial fluorescent reduction indicates that proteins indeed experience conformational changes to accommodate the phosphate buffered saline (PBS) environment.

Upon addition of neutral PEG to LYZ or BSA solutions at different PEG:BSA and LYZ:BSA mass ratios, tryptophan fluorescence increased from 9.8% to 14.5% for PEG:BSA systems (Fig. 1B1) and from 1.3% to 5% for PEG:LYZ systems (Fig. 1B2) as PEG:protein mass ratios increased from 0.5 to 16. As compared to tryptophan fluorescence in control experiments (without PEG) after 5 h, enhanced tryptophan fluorescence clearly demonstrates the existence of interactions between PEG and proteins. Particularly at high PEG:protein ratios of >4, the intensity of tryptophan fluorescence was only slightly reduced by 0.5–1% up to 24 h compared to that of tryptophan fluorescence at 0 h. This indicates that PEG is likely to play a protective role in retaining tryptophan's fluorescence by the formation of protein–PEG complexes. In contrast, in the presence of pSBMA, regardless of the amount of pSBMA added to LYZ or BSA protein solution, the fluorescence signals of proteins in the presence of pSBMA were almost identical to each other, and also close to that of proteins in the absence of pSBMA at the same time point (Fig. 1A1 and A2). The independence of fluorescence signals upon pSBMA addition clearly suggests no or undetectable interactions between pSBMA and proteins. Our and other works [44–47] have demonstrated experimentally and theoretically that zwitterionic pSBMA has a strong ability to form a hydration layer via ionic solvation, which will form a physical and energetic barrier to prevent interactions with proteins, leading to similar protein behavior in conformational changes in pure PBS solution and in pSBMA solutions. However, PEG, as a well-studied hydrophilic polymer, also exhibits amphiphilic characteristics at high molecular weight. A number of studies have also shown that several surface residues of LYZ, particularly Trp, involve nonspecific interactions (very likely to be hydrophobic interactions) with PEG [48–51]. Additionally, due to a certain degree of hydrophobic character, when proteins and PEG approach each other, a short-range protein–polymer attraction could also occur. A combination of these interactions makes Trp and its surrounding environments more hydrophobic, resulting in an increase of fluorescence signals as PEG amounts increase.

As shown in Fig. 1, the first 5 h is critical for monitoring fluorescence changes (i.e. protein conformation changes) upon incubation of proteins with polymers. Thus, we collected fluorescence intensity data for all protein–polymer systems at polymer:protein mass ratios (10:1) for every 1.5 h in the first 5 h. For any given pure protein or protein–polymer system, the relative fluorescence intensity ratios were obtained by normalizing the fluorescence intensity of different time points with respect to fluorescence intensity at 0 h (Fig. 2). It can be seen clearly that the fluorescence curves of pure protein systems were almost identical to those of pSBMA–protein systems, but exhibited significant differences from those of PEG–protein systems. This is further evidence that proteins are involved with interactions with PEG, causing fluorescence gain, but not with pSBMA. For all systems, the kinetics of the fluorescence intensity ratio were monotonically decreased with time, but BSA-involved systems had a relatively faster decrease in fluorescence ratio (Fig. 2A) than LYZ-involving systems (Fig. 2B), suggesting that flexible BSA undergoes a larger conformational change than rigid LYZ.

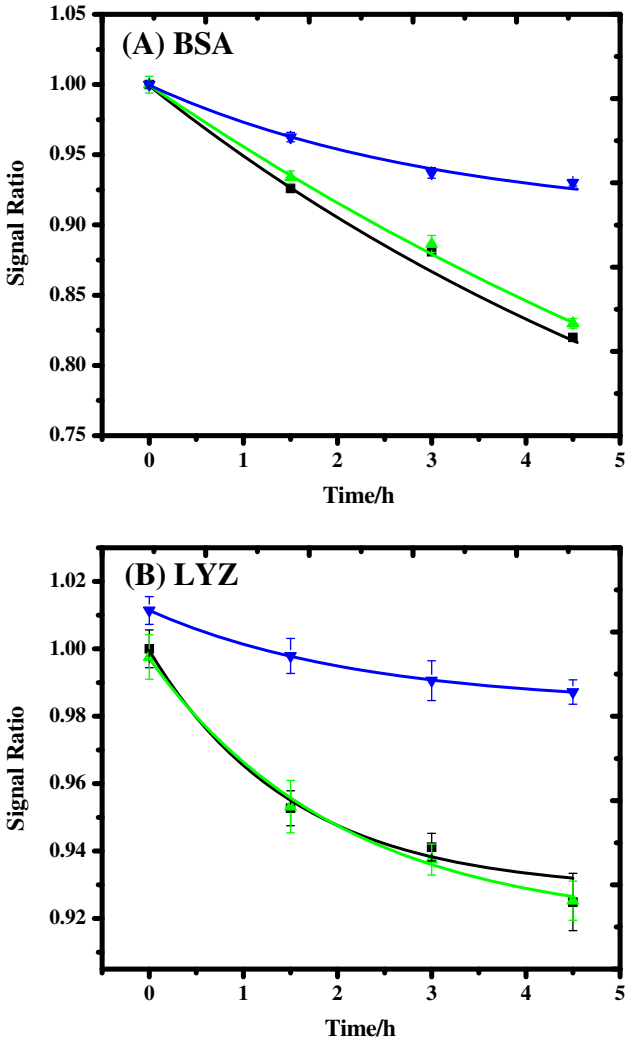

Fig. 2. Normalized fluorescence intensity of (A) BSA and (B) LYZ in the absence and presence of PEG and pSBMA at the first 5 h. Protein (■), protein–pSBMA (▲), protein–pEG (▼), ExpDec1Fit of protein (–), ExpDec1Fit of protein–pSBMA (–), ExpDec1Fit of Protein–pEG (–). Normalized fluorescence intensity is defined by a ratio of the fluorescence intensity of the polymer–protein mixture (10:1) at different time points with respect to the fluorescence intensity of pure protein at 0 h.

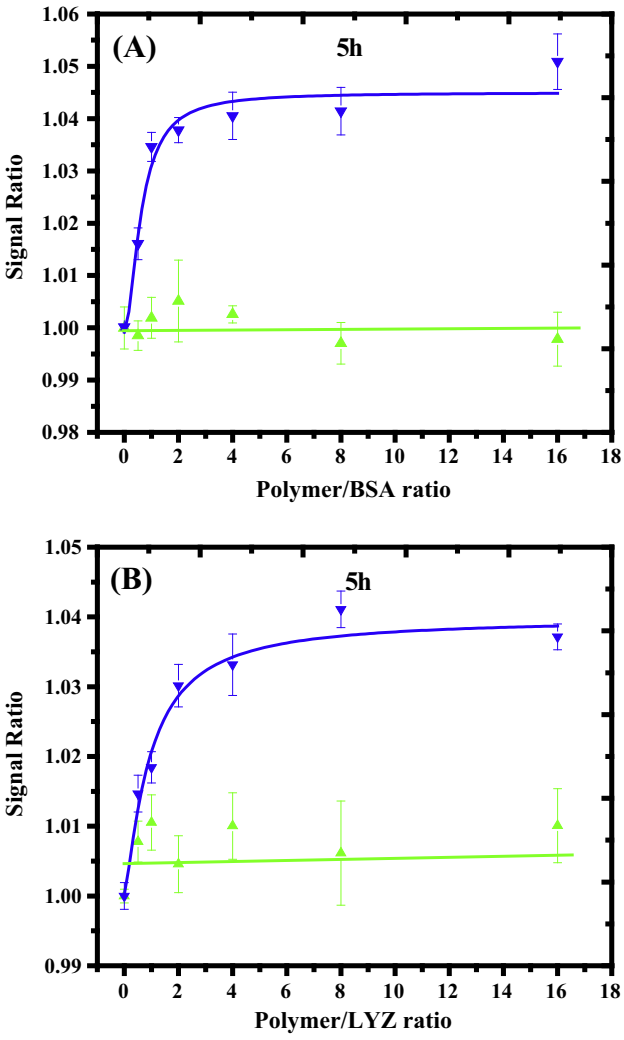

Fig. 3. Normalized fluorescence intensity of (A) BSA and (B) LYZ as a function of polymer:protein mass ratios at 5 h. Protein–pSBMA (▲), protein–pEG (▼), Hill 1Fit of protein–pEG (–). Normalized fluorescence intensity is defined by a ratio of the fluorescence intensity of the polymer–protein solutions at different polymer:protein ratios with respect to the fluorescence intensity of the pure corresponding protein solutions.

Tryptophan fluorescence data can be presented differently. Fig. 3 shows the effect of polymer:protein mass ratios on fluorescence change at 5 h. Consistent with the analysis above, the addition of different amounts of zwitterionic pSBMA into both BSA and LYZ protein solutions had almost no influence on the fluorescence change of proteins. In the presence of PEG, however, fluorescence signals increased rapidly and exponentially to a plateau at lower PEG/BSA ratios of <4 or at PEG/LYZ ratios of <8, and then remained there at higher PEG/protein ratios. The threshold PEG/protein ratios (PEG/BSA = 4 in Fig. 3A and PEG/LYZ = 8 in Fig. 3B) suggest a saturated concentration to form polymer–protein complexes. Large BSA requires more polymers and longer time to achieve saturated interactions during the unfolding process of proteins.

ANS fluorescence is further used to detect and quantify the exposed hydrophobic patches on proteins upon interacting with polymers. Since ANS dye displays enhanced fluorescence and a characteristic blue shift in its fluorescence emission maximum from 515 to 475 nm when bound to protein hydrophobic surfaces [52,53], ANS fluorescence is especially useful in detecting partially folded conformations of globular proteins. Fig. 4 shows an ANS fluorescence signal of BSA upon interacting with pSBMA or PEG at different time points. In the presence of pSBMA (Fig. 4A), ANS fluorescence of pSBMA–BSA mixtures with different ratios was similar to each other and to that of pure BSA at different time points (0, 5 and 24 h). ANS fluorescence results further confirm that BSA protein behavior is similar in the absence and presence of pSBMA, consistent with tryptophan fluorescence results. For PEG–BSA systems (Fig. 4B) at 0 h, regardless of PEG:BSA ratios from 0 to 16, ANS fluorescence remained almost constant, suggesting that PEG had not started to interact with BSA to induce conformational changes. But, at 5 and 24 h, fluorescence signals gradually increased as PEG:BSA ratios increased. The increase trend became more pronounced at longer incubation times of 24 h and higher PEG:BSA ratios of >4. This demonstrates an increased hydrophobic patch on the BSA surface for ANS to bind, when PEG-BSA interactions induce a slightly unfolded conformation of BSA that is very different from the initial conformation at 0 h. In all of the PEG-involved systems studied here, the increment in ANS fluorescence intensity correlates well with the increase in tryptophan fluorescence.

3.2. Monitoring the morphological changes of proteins induced by polymers

It is of interest to examine the morphological changes of proteins (BSA and LYZ) upon incubation with polymers (PEG and pSBMA). 2 μg ml^{-1} of protein or polymer–protein solution was incubated in the PBS bulk over 24 h, which provided enough time for the protein to interact with polymers in solution, prior to deposition on a HOPG surface for tests. Deposited samples were rinsed 10 times with 50 μl deionized water to remove any loosely bound polymers, proteins and protein/polymer complexes. The morphology of deposited aggregates firmly adsorbed on HOPG was then analyzed by tapping-mode AFM. For BSA-involved systems, some small and uniform sphere-like molecules of 5–8 nm were observed in pure BSA solution (Fig. 5A). Upon incubation of BSA with pSBMA, spherical particles similar in size, shape and quantity were clearly presented (Fig. 5B). Conversely, the mixture of BSA and PEG solution produced large, irregular-shaped strips, in sharp contrast to the morphologies of pure BSA and mixed BSA–pSBMA solutions (Fig. 5C). Additionally, the bundle strips of PEG–BSA were observed to have increased their lengths and adsorption densities, suggesting that PEG enables overall morphological changes and increase adsorption of BSA–PEG aggregates to be induced on the HOPG surface. Similar phenomena were also observed for the LYZ-involved systems. Pure LYZ and mixed LYZ–pSBMA show morphologically similar sphere-like molecules. This morphology was very different from the bundle-strip-like morphology of LYZ aggregates (Fig. 5D–F). The individual and scattered bundles had lengthened (up to 600 nm) and connected with each other to form a network. The formation of these bundle aggregates and their transformation into higher orders of aggregates from protein–pEG solutions are explainable by the intermolecular interactions of different noncovalent bonding forces between protein and PEG in a complementary manner. We should note that upon incubation of the protein–polymer bulk solution on the hydrophobic HOPG surface, the HOPG may also contribute to certain morphological changes of aggregates during the deposition and drying processes. Such HOPG-induced morphological changes are generally attributed to combination effects of geometrical confinement and surface hydrophobicity. Meanwhile, the drying process may also induce the conformational change of deposited protein–polymers/proteins/polymers, but this process will not greatly affect protein–polymer association if such complexes are already formed in solution. Thus, we expect that the morphologies observed should reflect the solution condition during the drying process. In addition, the AFM tip may induce the deformation to the scanned objectives regardless of whether the conditions are dry or wet. Overall, the qualitative AFM images provide additional evidence that PEG has a relatively stronger interaction with proteins than pSBMA, complementary to more quantitative results from NMR and fluorescence experiments. Similar morphologies between protein and protein–pSBMA systems and different morphologies between protein/protein–pSBMA and protein–pEG systems still indicate that the protein–pEG interactions in aqueous solution are most likely to induce the conformational changes of proteins, leading to different deposited morphologies.

3.3. Determining binding region between proteins and polymers

A 1-D ^{1}H-NMR study was also presented for determining the binding region between LYZ and polymers of PEG and pSBMA by large chemical shift changes upon titration with polymers. To monitor specific binding, PEG or pSBMA was titrated into a LYZ solution at ratios of 0, 0.5, 1 and 2:1. In Fig. 6A, upon complexation with PEG, chemical shift changes between 7.75 and 10.75 ppm were observed as PEG concentration increased, especially between 10.00 and 10.12 ppm, 8.78 and 8.89 ppm, 8.51 and 8.59 ppm and 8.00 and 8.13 ppm (Fig. 6C). According to Furness et al.'s work [48] and Redfield and Dobson's assignments [54], the maximal chemical shift changes occurred at the highest PEG concentration corresponding to the NH proton's signals of Glu-35, Arg-61, Trp-62, Arg-73, Lys-96 and Asp-101. However, no chemical shift changes were observed in the same range of 7.75–10.75 ppm upon pSBMA addition (Fig. 6B). The 1-D NMR chemical shift changes for the proton resonances were observed upon the direct binding of protein residues with polymers, which induced protein conformation changes and the associated microenvironment changes. As indicated by the clear chemical shift perturbation of the backbone NH signal of proteins upon adding with polymers (pSBMA and PEG), two distinct polymer behaviors suggest that these six residues containing Trp and Arg-rich residues form a hydrophobic binding core to interact with PEG. The indole side-chains of the tryptophan are essentially hydrophobic; although the guanidine groups of Arg carry positive charges, the propylene moieties of these residues are sufficiently hydrophobic enough to interact with PEG polymers. Furthermore, the visual inspection of the NMR-solved model structure (PDB: 1LYZ) [55] indicates that these six residues are located on the surface of LYZ (Fig. 6D), but separated by a relatively large distance between each other. To achieve potential binding between PEG and proteins, it is likely that long PEG chains are more favorable to intertwine and fold themselves to form this hydrophobic cluster and to interact with proteins via the formation of a protein corona. A previous NMR study of lysozyme binding to PEG by Furness et al. [48] also identified a hydrophobic binding site centered on Trp-62 and other binding residues involving Arg-61, Trp-63, Arg-73, Lys-96 and Asp-101. Consistently, the aromatic Trp-62 is found to be an important residue to interact with hydrophobic CH_2–CH_2 groups of PEG. But a comparison of our work and that of Furness et al. showed that Glu-35 and Trp-63 are different binding residues; this could be attributed to different molecular weights of PEG, experimental conditions and local and mutual conformational changes of proteins and PEG.

Taken together, numerous studies have demonstrated that both neutral PEG and zwitterionic pSBMA as superlow fouling materials exhibit very strong resistance to proteins, but our collective results from Trp fluorescence, ANS fluorescence, AFM and NMR confirm that within the criteria for superlow fouling materials (<0.3 ng cm^{-2} adsorbed proteins), PEG indeed involves nonspecific hydrophobic interactions with proteins in aqueous solution, and such interactions increase with PEG concentration due to the increased hydrophobicity of the longer PEG chain. This relatively strong interaction with protein is mainly attributed to multiple and steady contact points with proteins [48]. Additionally, the lower MW of PEG-4700 also showed the hydrophobic interaction between PEG and tryptophan of proteins, as indicated by fluorescence experiments and AFM results (data not shown). However, when the PEG MW was further reduced to 400, no hydrophobic interactions were observed, presumably because short PEG chains cannot adequately establish multiple contact points with proteins, resulting in either weak or no detectable interactions between PEG and proteins. As a wide use of biocompatible antifouling materials, the nature of weak PEG–protein interaction is often neglected, but in some applications of PEG-coated drug delivery carriers, PEG-functionalized proteins and enzyme, and biosensors with a PEG-inserted background, the very weak and reversible PEG–protein interaction is still sufficient enough to compromise the performance of PEGylated applications and devices. On the contrary, pSBMA possesses a true inert nature, and highly hydrated layers surrounding the opposing charges of zwitterionic quaternary ammonium cation and sulfonic acid groups create a high energy barrier to prevent the interaction with proteins. The

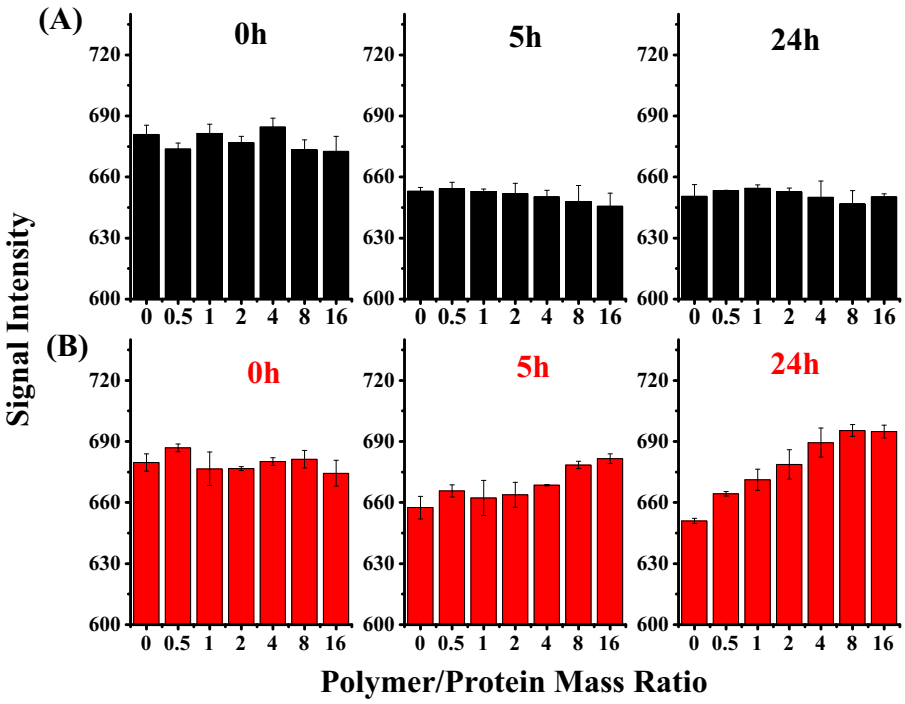

Fig. 4. Effect of polymer/protein mass ratio on ANS fluorescence intensity for (A) pSBMA–BSA and (B) PEG–BSA solutions at 0, 5 and 24 h.

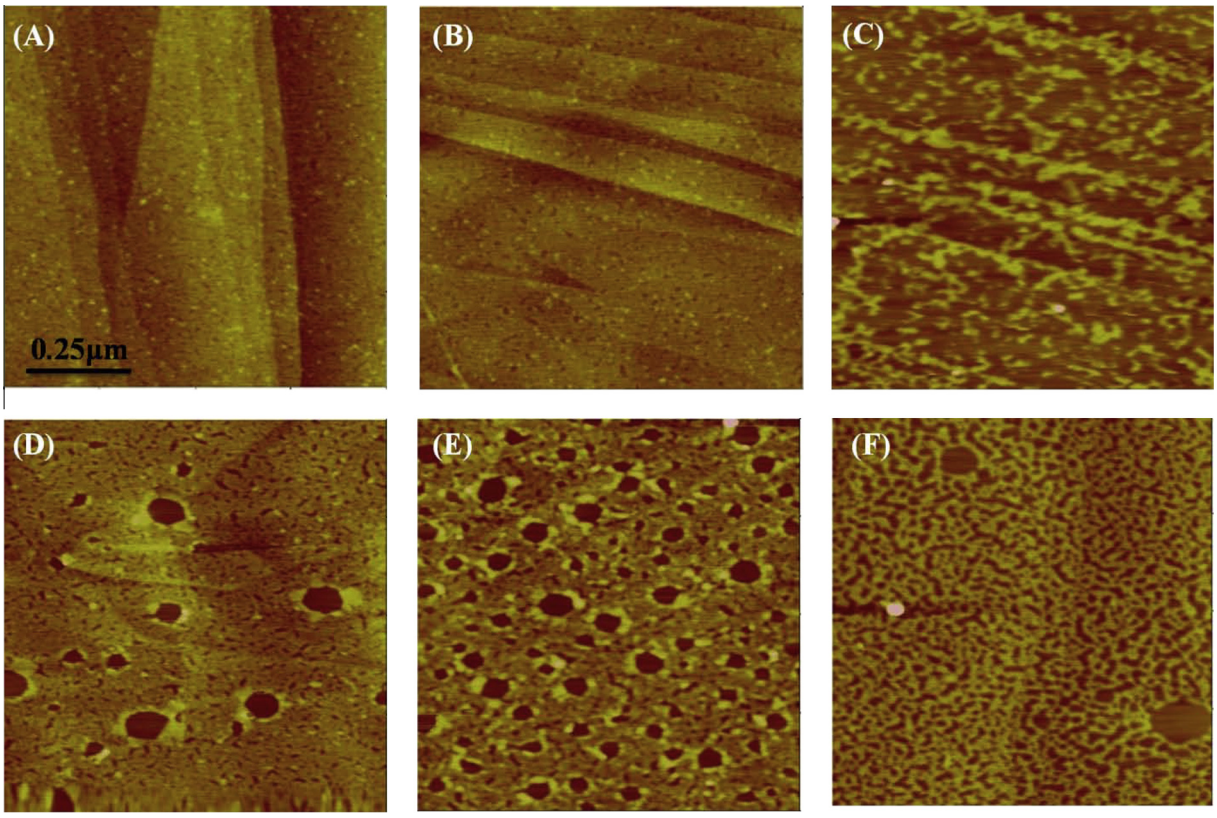

Fig. 5. AFM images of the HOPG surface soaked into different solutions: (A) BSA, (B) pSBMA–BSA, (C) PEG–BSA, (D) LYZ, (E) pSBMA–LYZ and (F) PEG-LYZ solutions on the HOPG.

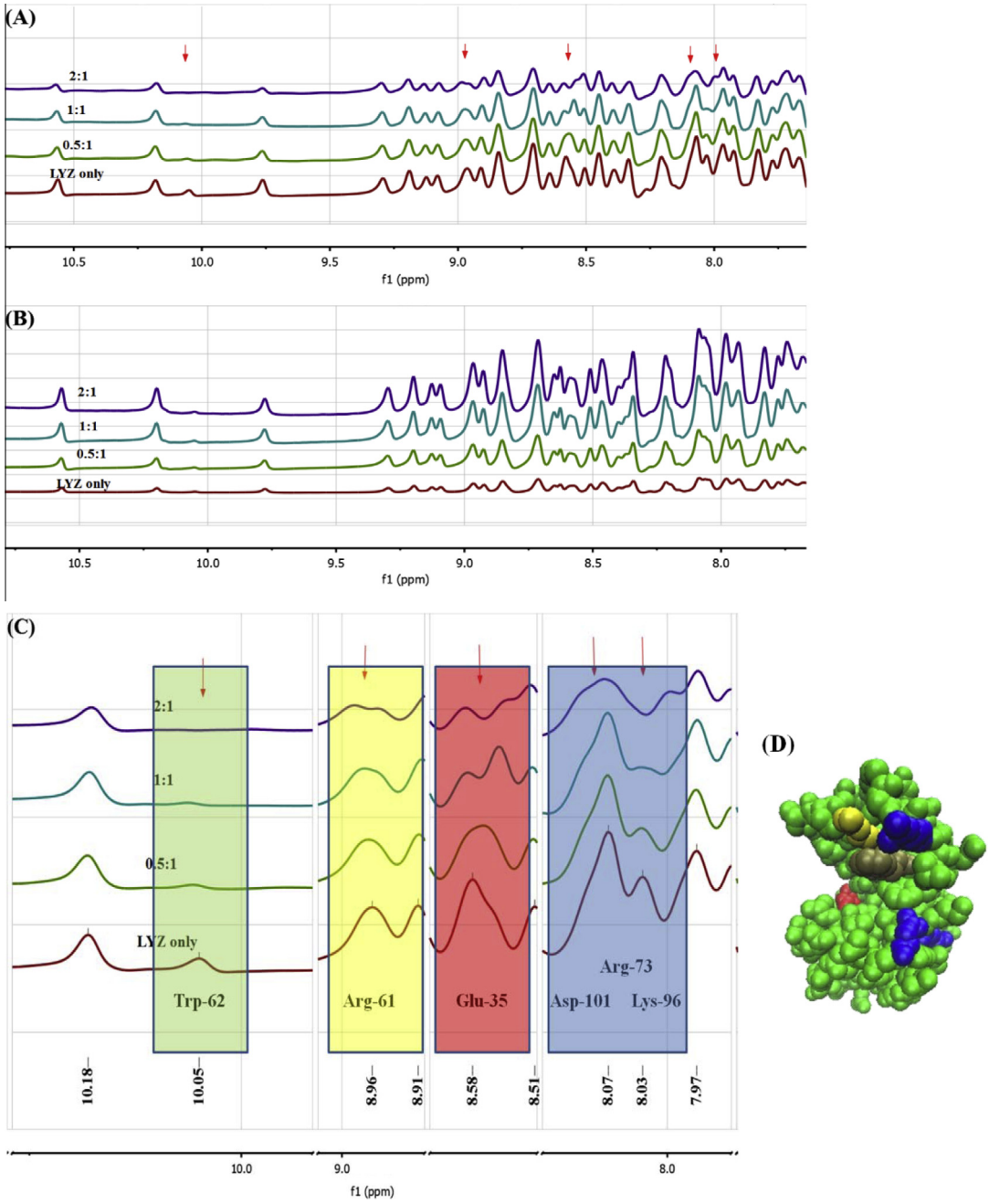

Fig. 6. Titration of low field LYZ ^{1}H-NMR signals upon incubation with (A) PEG, (B) pSBMA and (C) special magnified PEG. Chemical shift changes were assigned to binding residues (arrows). (D) Visual inspection of LYZ structure (PDB: 1LYZ) with PEG-binding residues of Arg-61 (yellow), Trp-62 (tan), Glu-35 (red), Asp-101, Arg-73 and Lys-96 (blue).

superior antifouling ability of pSBMA over PEG was also demonstrated by its better protein resistance ability, long-term structural stability and blood circulation time, in previous works by us and others [28,37].

4. Conclusions

In this work, we investigate the interaction of two model proteins (BSA and LYZ) with two antifouling polymers (neutral PEG and zwitterionic) in solution – a long-neglected problem – using tryptophan fluorescence, ANS fluorescence, AFM and NMR. Fluorescence data demonstrate that under different polymer:protein ratios tested, PEG indeed exhibits weak hydrophobic interactions with proteins in the aqueous solution, while pSBMA shows no or undetectable interactions with proteins. Morphological changes by AFM further confirm that both pure protein and mixed protein–pSBMA systems generate morphologically similar aggregates, in sharp contrast to the morphologies of PEG-induced protein aggregates. Furthermore, NMR data identify several preferred binding residues of Glu-35, Arg-61, Trp-62, Arg-73, Lys-96 and Asp-101 on the surface of lysozyme upon interacting with PEG, but not with pSBMA. Different interactions between proteins and PEG/pSBMA that have not been reported previously are likely attributed to their different surface hydration abilities, in which pSBMA can bind water molecules even more strongly via ionic solvation while PEG achieves hydration via hydrogen bonding. As

proof-of-concept experiments, this work prompts us to reconsider the effect of weak PEG–protein interactions, which are often either neglected or undetected, on many biological applications. To provide a more complete picture of protein–antifouling polymer interactions, ongoing studies are in progress to evaluate the effect of protein concentration, polymer molecular weight and solution composition on protein–polymer binding affinity and sites, and mutual changes in polymer and protein structure and dynamics.

Acknowledgements

We thank Dr Venkat Dudipala and Linlin Li for their assistance in NMR experiments. J.W. acknowledges financial support from a special foundation for an innovative talent training project of Zhejiang University (a part of the "985" program). S.C. thanks the National Nature Science Foundation of China (20974095, 20936005, and 21174127), the Zhejiang Provincial Natural Science Foundation of China (LZ13E030001) and the PhD Programs Foundation of Ministry of Education of China (20110101110034) for financial support. J.Z. thanks the National Science Foundation (CAREER Award CBET-0952624 and CBET-1158447) for financial support.

Appendix A. Figures with essential colour discrimination

Certain figures in this article, particularly Figs. 1–6 are difficult to interpret in black and white. The full colour images can be found in the on-line version, at http://dx.doi.org/10.1016/j.actbio.2013.09.038.

References

[1] Totrov M, Abagyan R. Flexible protein–ligand docking by global energy optimization in internal coordinates. Proteins Struct Funct Genet 1997;29:215–20.
[2] Looger LL, Dwyer MA, Smith JJ, Hellinga HW. Computational design of receptor and sensor proteins with novel functions. Nature 2003;423:185–90.
[3] Watanabe N, Madaule P, Reid T, Ishizaki T, Watanabe G, Kakizuka A, et al. P140mDia, a mammalian homolog of Drosophila diaphanous, is a target protein for Rho small GTPase and is a ligand for profilin. EMBO J 1997;16:3044–56.
[4] Wang W, Donini O, Reyes CM, Kollman PA. Biomolecular simulations: recent developments in force fields, simulations of enzyme catalysis, protein–ligand, protein–protein, and protein–nucleic acid noncovalent interactions. Annu Rev Biophys Biomol Struct 2001;30:211–43.
[5] Ruoslahti E, Pierschbacher MD. New perspectives in cell adhesion: RGD and integrins. Science 1987;238:491–7.
[6] Stolnik S, Dunn SE, Garnett MC, Davies MC, Coombes AG, Taylor D, et al. Surface modification of poly(lactide-co-glycolide) nanospheres by biodegradable poly(lactide)–poly(ethylene glycol) copolymers. Pharm Res 1994;11:1800–8.
[7] Jiang S, Cao Z. Ultralow-fouling, functionalizable, and hydrolyzable zwitterionic materials and their derivatives for biological applications. Adv Mater 2010;22:920–32.
[8] Ishihara K, Fukumoto K, Iwasaki Y, Nakabayashi N. Modification of polysulfone with phospholipid polymer for improvement of the blood compatibility. Part 2. Protein adsorption and platelet adhesion. Biomaterials 1999;20:1553–9.
[9] Zhao C, Zheng J. Synthesis and characterization of poly(N-hydroxyethylacrylamide) for long-term antifouling ability. Biomacromolecules 2011;12:4071–9.
[10] Liu S, Kim JT, Kim S. Effect of polymer surface modification on polymer–protein interaction via hydrophilic polymer grafting. J Food Sci 2008;73:E143–50.
[11] Baszkin A, Lyman DJ. The interaction of plasma proteins with polymers. I. Relationship between polymer surface energy and protein adsorption/desorption. J Biomed Mater Res 1980;14:393–403.
[12] Knoll D, Hermans J. Polymer-protein interactions. Comparison of experiment and excluded volume theory. J Biol Chem 1983;258:5710–5.
[13] Yin L, Zhao Z, Hu Y, Ding J, Cui F, Tang C, et al. Polymer–protein interaction, water retention, and biocompatibility of a stimuli-sensitive superporous hydrogel containing interpenetrating polymer networks. J Appl Polym Sci 2008;108:1238–48.
[14] Holmlin RE, Chen X, Chapman RG, Takayama S, Whitesides GM. Zwitterionic SAMs that resist nonspecific adsorption of protein from aqueous buffer. Langmuir 2001;17:2841–50.
[15] Ladd J, Zhang Z, Chen S, Hower JC, Jiang S. Zwitterionic polymers exhibiting high resistance to nonspecific protein adsorption from human serum and plasma. Biomacromolecules 2008;9:1357–61.
[16] Chen S, Liu L, Jiang S. Strong resistance of oligo (phosphorylcholine) self-assembled monolayers to protein adsorption. Langmuir 2006;22:2418–21.
[17] Aguilar MR, Gallardo A, Lechuga LM, Calle A, San Román J. Modulation of proteins adsorption onto the surface of chitosan complexed with anionic copolymers. Real time analysis by surface plasmon resonance. Macromol Biosci 2004;4:631–8.
[18] Zhao C, Li L, Wang Q, Yu Q, Zheng J. Effect of film thickness on the antifouling performance of poly(hydroxy-functional methacrylates) grafted surfaces. Langmuir 2011;27:4906–13.
[19] Yang W, Chen S, Cheng G, Vaisocherová H, Xue H, Li W, et al. Film thickness dependence of protein adsorption from blood serum and plasma onto poly(sulfobetaine)-grafted surfaces. Langmuir 2008;24:9211–4.
[20] Tan KY, Lin H, Ramstedt M, Watt FM, Huck WT, Gautrot JE. Decoupling geometrical and chemical cues directing epidermal stem cell fate on polymer brush-based cell micro-patterns. Integr Biol 2013;5:899–910.
[21] Rodriguez Emmenegger C, Brynda E, Riedel T, Sedlakova Z, Houska M, Alles AB. Interaction of blood plasma with antifouling surfaces. Langmuir 2009;25:6328–33.
[22] Zhao C, Li L, Zheng J. Achieving highly effective nonfouling performance for surface-grafted poly(HPMA) via atom-transfer radical polymerization. Langmuir 2010;26:17375–82.
[23] Bernards MT, Cheng G, Zhang Z, Chen S, Jiang S. Nonfouling polymer brushes via surface-initiated, two-component atom transfer radical polymerization. Macromolecules 2008;41:4216–9.
[24] Jeon SI, Lee JH, Andrade JD, De Gennes PG. Protein–surface interactions in the presence of polyethylene oxide: I. Simplified theory. J Colloid Interface Sci 1991;142:149–58.
[25] Szleifer I. Protein adsorption on surfaces with grafted polymers: a theoretical approach. Biophys J 1997;72:595–612.
[26] Irvine D, Mayes A, Satija S, Barker J, Sofia-Allgor S, Griffith L. Comparison of tethered star and linear poly(ethylene oxide) for control of biomaterials surface properties. J Biomed Mater Res 1998;40:498–509.
[27] Gombotz WR, Guanghui W, Horbett TA, Hoffman AS. Protein adsorption to poly(ethylene oxide) surfaces. J Biomed Mater Res 2004;25:1547–62.
[28] Keefe AJ, Jiang S. Poly(zwitterionic)protein conjugates offer increased stability without sacrificing binding affinity or bioactivity. Nat Chem 2012;4:59–63.
[29] Cheng G, Zhang Z, Chen S, Bryers JD, Jiang S. Inhibition of bacterial adhesion and biofilm formation on zwitterionic surfaces. Biomaterials 2007;28:4192–9.
[30] Jiang S, Cao Z. Ultralow-fouling, functionalizable, and hydrolyzable zwitterionic materials and their derivatives for biological applications. Adv Mater 2010;22:920–32.
[31] Chen S, Li L, Zhao C, Zheng J. Surface hydration: principles and applications toward low-fouling/nonfouling biomaterials. Polymer 2010;51:5283–93.
[32] Zhao C, Li L, Guo M, Zheng J. Functional polymer thin films designed for antifouling materials and biosensors. Chem Pap 2012;66:323–39.
[33] He Y, Hower J, Chen S, Bernards MT, Chang Y, Jiang S. Molecular simulation studies of protein interactions with zwitterionic phosphorylcholine self-assembled monolayers in the presence of water. Langmuir 2008;24:10358–64.
[34] Hower JC, Bernards MT, Chen S, Tsao H-K, Sheng Y-J, Jiang S. Hydration of "nonfouling" functional groups. J Phys Chem B 2008;113:197–201.
[35] Greenwald RB, Choe YH, McGuire J, Conover CD. Effective drug delivery by PEGylated drug conjugates. Adv Drug Deliv Rev 2003;55:217–50.
[36] Chapman AP. PEGylated antibodies and antibody fragments for improved therapy: a review. Adv Drug Deliv Rev 2002;54:531–45.
[37] Lin W, Zhang H, Wu J, Wang Z, Sun H, Yuan J, et al. A novel zwitterionic copolymer with a short poly(methyl acrylic acid) block for improving both conjugation and separation efficiency of a protein without losing its bioactivity. J Mater Chem B 2013;1:2482–8.
[38] Tagami T, Uehara Y, Moriyoshi N, Ishida T, Kiwada H. Anti-PEG IgM production by siRNA encapsulated in a PEGylated lipid nanocarrier is dependent on the sequence of the siRNA. J Controlled Release 2011;151:149–54.
[39] Wu J, Wang Z, Lin W, Chen S. Investigation of the interaction between poly(ethylene glycol) and protein molecules using low field nuclear magnetic resonance. Acta Biomater 2013;9:6414–20.
[40] Baty AM, Suci PA, Tyler BJ, Geesey GG. Investigation of mussel adhesive protein adsorption on polystyrene and poly(octadecyl methacrylate) using angle dependent XPS, ATR-FTIR, and AFM. J Colloid Interface Sci 1996;177:307–15.
[41] Orasanu A, Bradley R. AFM and XPS study on albumin adsorption onto graphite surfaces. Eur Cell Mater 2003;6:46.
[42] Yang Z, Galloway JA, Yu H. Protein interactions with poly(ethylene glycol) self-assembled monolayers on glass substrates: diffusion and adsorption. Langmuir 1999;15:8405–11.
[43] Wu Z, Zhang X, Zhang X, Li G, Sun J, Zhang Y, et al. Nanobubbles influence on BSA adsorption on mica surface. Surf Interface Anal 2006;38:990–5.
[44] Shao Q, He Y, Jiang S. Molecular dynamics simulation study of ion interactions with zwitterions. J Phys Chem B 2011;115:8358–63.
[45] Wu J, Lin W, Wang Z, Chen S, Chang Y. Investigation of the hydration of nonfouling material poly(sulfobetaine methacrylate) by low-field nuclear magnetic resonance. Langmuir 2012;28:7436.

[46] Chen S, Jiang S. An new avenue to nonfouling materials. Adv Mater 2008;20:335–8.
[47] Chang Y, Chen S, Zhang Z, Jiang S. Highly protein-resistant coatings from well-defined diblock copolymers containing sulfobetaines. Langmuir 2006;22:2222–6.
[48] Furness EL, Ross A, Davis TP, King GC. A hydrophobic interaction site for lysozyme binding to polyethylene glycol and model contact lens polymers. Biomaterials 1998;19:1361–9.
[49] Israelachvili J. The different faces of poly(ethylene glycol). Proc Nat Acad Sci 1997;94:8378–9.
[50] Ragi C, Sedaghat-Herati M, Ouameur AA, Tajmir-Riahi H. The effects of poly(ethylene glycol) on the solution structure of human serum albumin. Biopolymers 2005;78:231–6.
[51] Bloustine J, Virmani T, Thurston G, Fraden S. Light scattering and phase behavior of lysozyme-poly(ethylene glycol) mixtures. Phys Rev Lett 2006;96:087803.
[52] Qu P, Wang Y, Wu G, Lu Z, Xu M. Effect of polyethylene glycols on the alkaline-induced molten globule intermediate of bovine serum albumin. Int J Biol Macromol 2012;51:97–104.
[53] Sen D, Mandal DK. Pea lectin unfolding reveals a unique molten globule fragment chain. Biochimie 2011;93:409–17.
[54] Redfield C, Dobson CM. Sequential proton NMR assignments and secondary structure of hen egg white lysozyme in solution. Biochemistry 1988;27:122–36.
[55] Diamond R. Real-space refinement of the structure of hen egg-white lysozyme. J Mol Biol 1974;82:371–91.